Journal of Solid State Electrochemistry (2018) 22:1507–1515
https://doi.org/10.1007/s10008-017-3840-8

ORIGINAL PAPER

Electrochromic and spectroelectrochemical properties of polythiophene β-substituted with alkyl and alkoxy groups

Luiza De Lazari Ferreira [1] · Hállen Daniel Rezende Calado [1]

Received: 14 July 2017 / Revised: 14 November 2017 / Accepted: 16 November 2017 / Published online: 30 November 2017

Abstract

Polythiophenes are conjugated polymers that are highly promising candidates for use as an active layer in flexible optoelectronic devices. The β-substitution position in the thiophene ring minimizes the occurrence of couplings during polymerization, producing more regular structures and resulting in better properties. The relatively high stability and the possibility of tuning the properties by molecular engineering make polythiophenes one of the most versatile classes of conjugated polymers. In this study, we present an investigation of the influence of two types of polythiophenes on their spectroelectrochemical properties: (i) poly(alcoxythiophenes) (POTs), including poly(3-methoxythiophene) (PMOT) and poly(3,4-ethylenedioxythiophene) (PEDOT), and (ii) poly(3-alkylthiophenes) (PYTs), including poly(3-hexylthiophene) (P3HT) and poly(3-dodecylthiophene) (PDDT). The polymers were electrochemically synthesized by cyclic voltammetry and characterized by infrared spectroscopy. The "in situ" simultaneous optical absorption and fluorescence investigation of the solutions showed new energy state polarons in the redox process. Chronoabsorptometry measurements enabled determination of parameters such as electrochromic efficiency, coulombic efficiency, optical contrast, and switching time of the polymers in the reduced and oxidized states. A switching time of 2 s and an electrochemical efficiency of almost 90 $cm^2\ C^{-1}$ are promising for applying these polymers in electrochromic devices.

Keywords Substituted polythiophenes · Electrochemistry · Electrochromism

Introduction

The high global demand for energy production and the urgent efforts to reduce environmental impact have led to a growing interest in research related to the use of solar energy with a lower cost and greater efficiency [1, 2].

Electrochromic devices (EDs) present a good alternative in this scenario due to their low power consumption [3, 4]. In addition, electrochromic materials are optically active materials characterized by reversible changes and optical properties in response to electrochemical changes [5, 6]. These materials are also promising because of the good optical contrast between their different color states, optical memory, stability to ultraviolet rays, thermal stability over different temperature ranges, and short switching time for optical changes [7, 8]. EDs have several applications, including intelligent windows [9], displays [10], and sunglasses [11]. In addition, conjugated polymers (CPs) have high-performance characteristics for application in EDs, such as high optical contrast in a short switching time [12], high redox stability and low processing cost [13, 14], and they are considered to be among the most applicable electrochromic materials due to their multicolor states in response to an applied potential [15, 16]. Polythiophene, polypyrrole, polyaniline, and their derivatives are typical examples of remarkable electrochromic CPs reported in the literature [17, 18].

Polythiophene (PT) forms a representative class of CPs with the potential for ED application due to its high thermal and environmental stability, organic solvent solubility, ease of processing, electrochromism, and good electrochemical stability [11, 13, 19]. β-substituted PTs present more regular structures and better properties due to the minimization of couplings between the polymer chains during chemical or electrochemical synthesis [20].

✉ Luiza De Lazari Ferreira
luizadl@yahoo.com.br

✉ Hállen Daniel Rezende Calado
hallendaniel@yahoo.com.br

[1] Departamento de Química, ICEx - Universidade Federal de Minas Gerais, Belo Horizonte, Brazil

In the current study, four β-substituted derivatives of PTs were synthesized, namely, two poly(3-alkoxythiophenes) (POTs) of poly(3-methoxythiophene) (PMOT) and poly(3,4-ethylenedioxythiophene) (PEDOT) and two poly(3-alkylthiophenes) (PYTs) of poly(3-hexylthiophene) (P3HT) and poly(3-dodecylthiophene) (PDDT). The synthesis involved electrochemical polymerization with cyclic voltammetry (CV) in acetonitrile with sodium perchlorate ($NaClO_4$) as the electrolyte. The structural and electrochemical properties of the polymers were investigated using Fourier transform infrared spectroscopy (FTIR) and CV, respectively. Chronoabsorptometry and spectroelectrochemical measurements revealed the potential for ED application of these materials by determining parameters such as optical contrast, switching time, and coloration efficiency. The influences of the thiophene ring substituent groups on these properties were determined due to the presence of the oxygen atom in the alkoxythiophenes and the alkyl chain length of the alkylthiophenes.

Experimental

Materials

The monomers 3-metoxythiophene (MOT), 3,4-ethylenedioxythiophene (EDOT), 3-hexylthiophene (3HT), and 3-dodecylthiophene (DDT) were purchased from Sigma-Aldrich Co. and used as received. Sodium perchlorate ($NaClO_4$, electrochemical grade) and tetrabutylammonium perchlorate (TBAP, electrochemical grade) were obtained from Aldrich and Fluka Co., respectively. The acetonitrile (AN) (99.8%) solvent was dried in a previously activated [21] molecular sieve of 3 Å (10% *m*/*v*). Tetrahydrofuran (THF) was purchased from Vetec. All measurements were conducted in a nitrogen atmosphere (N_2).

Glass recovered with indium tin oxide (ITO)-doped substrate was obtained from Delta Technologies (8–12 Ω; 7.0 mm × 50.0 mm × 0.7 mm).

Instrumentation

FTIR spectra were recorded for all samples in powder form on a Thermo Scientific Nicolet 380 spectrometer using attenuated total reflectance (ATR, ZnSe crystals). The emission and absorption spectra were recorded on a Varian Cary Eclipse spectrofluorimeter and a UV-Vis Cary 100 Bio spectrophotometer, respectively.

The surface morphology of the polymer films was studied via scanning electron microscopy (SEM) on a Superscan Schimadzu SSX-550 instrument.

The electrochemical experiments were performed using a Palmsens potentiostat. These experiments were performed at room temperature.

Computer-controlled spectroelectrochemical measurements were performed using a UV-Visible Cary 100 Bio spectrometer connected to an Autolab PGSTAT204 instrument.

Electrochemical experiments

The electrochemical experiments were conducted in a typical three-electrode cell (~2 mL). A disk platinum electrode (a = 1.13 10^{-2} cm^2) was used as the working electrode (WE), a platinum wire was used as the counter electrode (CE), and Ag/Ag^+ was used as the quasi-reference electrode (RE). The electrochemical experiments were conducted using a potentiostat Palm Sens. All measurements were performed under an inert nitrogen (N_2) atmosphere.

Firstly, CV measurements were recorded at a scan rate of 50 mV s^{-1} using a low monomer concentration (2.0 mmol L^{-1}) to avoid polymer formation. The redox profile of POT was studied in distilled water/acetonitrile (3:1) containing 0.1 mol L^{-1} of $NaClO_4$ and that of PYT in AN containing 0.1 mol L^{-1} of $NaClO_4$.

Polymeric POT films were obtained by CV using a solution of 35 mmol L^{-1} of the monomer in water/acetonitrile (3:1) in the range of − 0.5 to 1.5 V vs Ag/Ag^+. Polymeric PYT films were obtained by CV using a solution of 0.1 mol L^{-1} of the monomer in AN in the range of 0.5 to 1.6 V vs Ag/Ag^+. After polymerization, the films were rinsed with AN, and the electrode was transferred to one of the cells containing the corresponding electrolyte solution free monomer for which the redox profile of the polymeric film was submitted to different scanning speeds (10, 20, 50, 75, 100, and 150 mV s^{-1}).

Spectroelectrochemical experiments

The polymer films were obtained on ITO-coated glass (Delta Technologies; 7 × 50 × 50 mm, $8 \leq R \geq 12$ Ω) by chronopotentiometry deposition (2 mA cm^{-2}, 20 s for POT and 40 s for PYT) using monomer solutions 0.1 mol L^{-1} in nitrobenzene ($ØNO_2$) containing tetrabutylammonium tetrafluoroborate (Bu_4NBF_4) (0.1 mol L^{-1}). After the deposition, the films were rinsed with distilled water and inserted in an electrochemical cell. The higher ITO resistance compared to Pt implied the electrolyte change and a more rigorous kinetic control (low temperature ~ 5 °C) to obtain homogeneous thin films.

The electrochemical cell was assembled in a standard quartz cuvette (1 cm × 1 cm) using ITO as the WE, a Pt wire as the counter electrode, and a Pt wire as a quasi-reference. The cuvette was filled with the supporting electrolyte solution (0.1 mol L^{-1} Bu_4NBF_4 in AN solution). Spectroelectrochemical experiments were performed on the electrochemical cell that

was inserted in the spectrophotometer UV Cary 100 Bio connected to an Autolab Potentiostat/Galvanostat (PGSTAT 204). The films were stabilized in the electroactivity range of each material at increasingly positive potentials with increments of 0.1 V, and after each current signal was stabilized, one absorption spectrum was recorded. The absorbance was measured between 300 and 800 nm at a constant potential while a stable current was achieved (constant E value for 60 s).

The chronoabsorptometry experiments were performed using the same experimental apparatus as that described for spectrolectrochemical examination. The film was subjected to ten potential jumps between the states of oxidation and reduction by chronoamperometry accompanied by UV-Vis transmittance measurement.

Optical experiments

The polymer solution was prepared by dissolving 1 mg of polymer into 3 mL of THF solvent and stirring for more than 4 h. Absorption spectra were recorded for each sample. Fluorescence spectra were obtained with excitation at the maximum absorption of each polymer. Both measurements were performed in solution in a quartz cuvette (1 cm × 1 cm).

Results and discussion

FTIR-ATR spectroscopy

The FTIR-ATR spectra obtained for POT and PYT are shown in Fig. 1. All of the obtained spectra present bands characteristic of the expected structures for the prepared polymers.

The absorptions for the asymmetric and symmetric stretching modes of the methylene groups are shown in the infrared spectra, respectively, at 2928 and 2857 cm^{-1} for PMOT; 2925 and 2851 cm^{-1} for PEDOT; 2916 and 2856 cm^{-1} for P3HT; and 2916 and 2843 cm^{-1} for PEDOT. This region of the spectrum has an –C–S asymmetric stretching contribution. The higher intensity of these signals for the PYTs is attributed to the alkyl substituent chain on the thiophene ring [22]. The bands at 1355 cm^{-1} (PMOT), 1358 cm^{-1} (PEDOT), 1348 cm^{-1} (P3HT), and 1339 cm^{-1} (PDDT) were attributed to bending deformations of the –C–H groups. The absorptions at 1086 cm^{-1} (PMOT) and 1094 cm^{-1} (PEDOT) were attributed to C–O–C stretching with a contribution from the $=C_{\beta}$–H band. The out-of-plane stretching of the alkyl chain (CH_2) of PYT appears around 1077 cm^{-1}. The characteristic C–S stretching peak of the PT ring appeared for PMOT, PEDOT, P3HT, and PDDT at 810, 840, 824, and 818 cm^{-1}, respectively, providing evidence of the polymer formation [23].

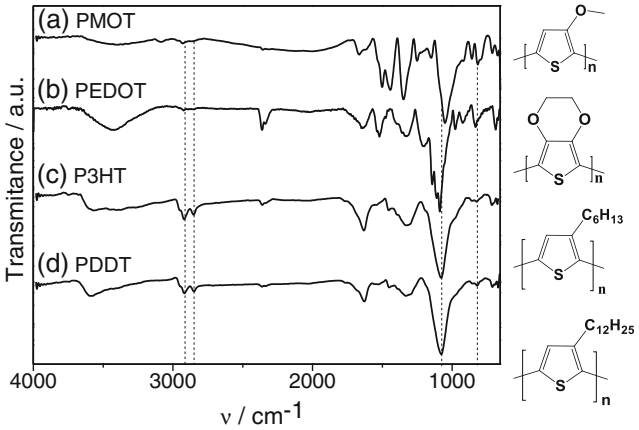

Fig. 1 Spectra in the infrared region (FTIR-ATR) for the following: **a** PMOT, **b** PEDOT, **c** P3HT, and **d** PDDT

Electrochemical characterization

Figure 2 shows the voltammograms obtained for the samples at different scanning speeds. All of the polymers showed quasi-reversible behavior at the speeds studied. PYT and POT exhibited a well-defined oxidation peak and reduction peak, at minimum.

The CV curves for the polymers in Fig. 2 show only a redox peak, indicating that the capacitance of these materials primarily results from the double-layer capacitance. The PEDOT presented capacitive behavior that was attributed to the high electronic density present in its structure, which was associated with the direct attachment of oxygen to the thiophene ring. The PMOT polymer exhibited a considerably higher oxidation potential (0.4 V greater, Fig. 2b) than PEDOT, possibly attributed to a large torsion angle between the repeated units in the electroneutral polymer chain [24].

From the voltammetric curves obtained at 20 mV s^{-1}, the thermodynamic variables are presented in Table 1. The heteroatom plays an important role in the electrochemical behavior of the CPs through p-π * and π-π *type transitions, causing a reduction in the oxidation potential. Therefore, the polymerization conditions become gentler, which favors the formation of polymers with better regioregularity properties [25]. This behavior was observed for POT, PMOT, and PEDOT, which presented lower values than PYT, P3HT, and PDDT of anode peak potential (E_{pa}).

The values for $\Delta E_{p/2}$ were determined by the average value of the anodic and cathodic peak potentials. The value of $\Delta E_{p/2}$ is related to the existence of an anodic residual current in the voltammograms, which is generally attributed to the double-layer charge in the oxidized conductive polymer.

The reaction scheme of the redox process can be described as follows:

$$P + X^- \overset{E^{0\prime}}{\longleftrightarrow} P^+X^- + e^-$$

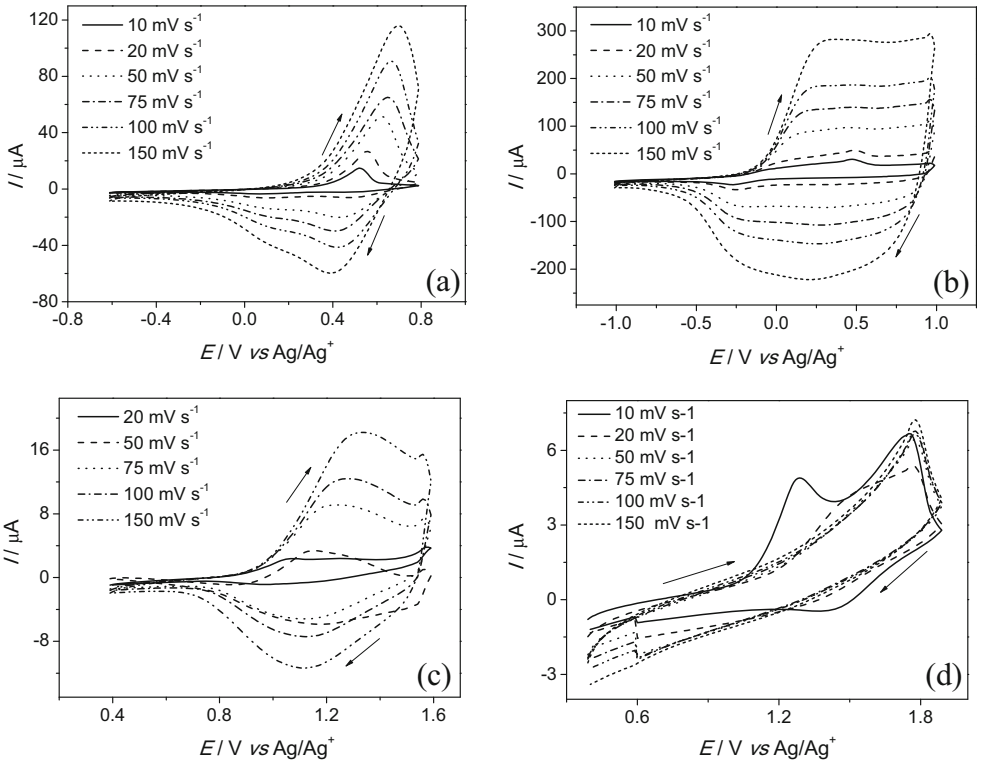

Fig. 2 Cyclic voltammogram for **a** PMOT, **b** PEDOT, **c** P3HT, and **d** PDDT at different scanning speeds. WE = CE = Pt, RE = Ag/Ag^+. Electrolyte: $NaClO_4$ 0.1 mol L^{-1}/AN

where P is approximately equal to 3 monomeric units. Considering the values obtained at 20 mV s^{-1}, it was observed that $E^{0\prime}$ is higher for alkyl than for alkoxy substituents. The $E^{0\prime}$ value for PEDOT is lower than that for PMOT because of the mesomeric and inductive donor effects of the two oxygenated substituents [25]. For PYT, the value of $E^{0\prime}$ increases as the size of the alkyl substituent chain increases due to the steric effect of the alpha helix. In addition, the length of the polymer chain also influences the value of $E^{0\prime}$. A more CP has a lower redox potential value, so that its electrons become more delocalized and more easily oxidized. According to the results obtained, PEDOT presents a greater extent of conjugation, followed by PMOT, P3HT, and PDDT.

Table 1 Summary of voltammetric data for the curves obtained at 20 mV s^{-1}

Polymer	E_{pa}/ V	E_{pc}/ V	I_{pa}/µA	$E^{0\prime}$/ V	$\Delta E_{P/2}$/ V
PMOT	0.55	0.46	27.50	0.50	0.09
PEDOT	0.15	0.29	11.56	0.22	0.14
P3HT	1.07	0.97	2.41	1.02	0.10
PDDT	1.49	1.01	144.22	1.25	0.45

WE = CE = Pt, RE = Ag/Ag^+. Electrolyte 0.1 mol L^{-1} $NaClO_4$/AN

Anodic (E_{pa}) and cathodic (E_{pc}) peak potentials; anodic (I_{pa}) peak current; formal redox potential ($E^{0\prime} = E_{pa} + E_{pc}$)/2; width at half height of normal peak ($\Delta E_{p/2} = |E_{pa} - E_{pc}|$)

All polymers showed an anodic potential dependence on the scan rate, which denoted a quasi-reversible profile, as displayed in Fig. 3. Small variations of the anodic peak potential as a function of the scanning velocity can be related to the ohmic drop due to the ionic conductivity as the solvent decreased with increasing speed.

Plots of the anodic peak current as a function of scan rate for POT and PYT were nearly linear, denoting redox reactions with superficial reactions and negligible mass transport [26, 27] (Fig. 3). The experimental data do not pass through the origin, indicating the presence of residual current.

Optical characterization

When the material is excited, the absorbed photon has more energy than the forbidden band of the semiconductor, thus tending to enter into an energy balance with the solution; due to this effect, the minimum energy is reached through the emission of phonons [28]. From the curves shown in Fig. 4, it can be observed that all of the reduced materials possess an absorption band due to a transition from the valence band to the conduction band (VB → CB) near 400 nm (3.1 eV).

The optical absorption of PMOT (Fig. 4a) presented two absorption bands of violet and blue at 289 nm (4.29 eV) and 486 nm (2.55 eV), respectively, which could be attributed to n→π* transitions associated with the presence of the oxygen heteroatom in its structure and the π→π* of the thiophene

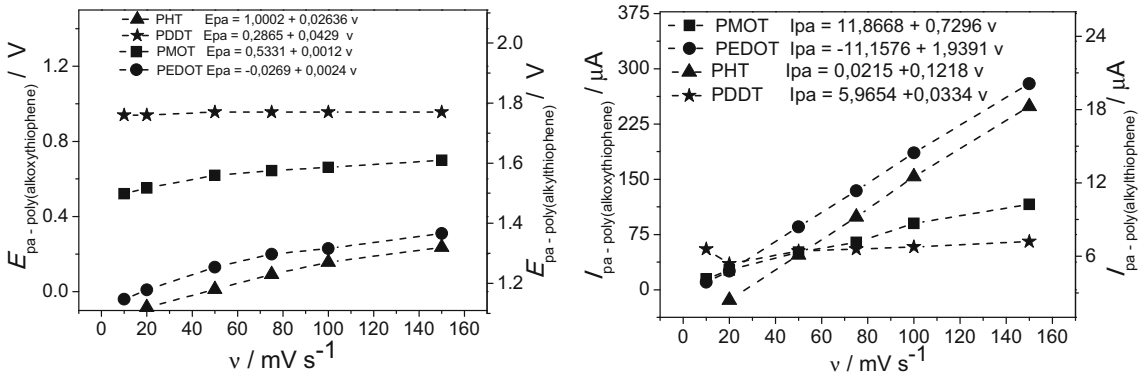

Fig. 3 Left: variation of anode peak potential (E_{pa}) as a function of scanning speed. Right: variation of the anodic peak current (I_{pa}) as a function of scanning speed for poly(alkoxythiophenes) and poly(3-alkylthiophenes). WE = CE = Pt, RE = Ag/Ag^+. Electrolyte: $NaClO_4$ 0.1 mol L^{-1}/AN

ring. For this sample, a maximum emission was identified in orange at 568 nm (2.18 eV). In Fig. 4b, PEDOT presented an optical absorption at 529 nm (2.34 eV) and a maximum emission at 647 nm (1.92 eV). The polymers P3HT (Fig. 4c) and PDDT (Fig. 4d) presented similar spectra with absorptions and emissions in the same region, which are associated with the similarity of the structures. These samples presented an absorption of violet with a maximum near 412 nm (3.01 eV) and an emission of orange at ~ 568 nm (2.18 eV). For PDDT, a bathochromic shift (displacement for a longer wavelength-red region of the electromagnetic spectrum) was expected compared with P3HT due to the inductive effect of the polymer chain increase, but this displacement was not detected.

A difference in the absorption region between the poly(alkoxythiophenes) and poly(3-alkylthiophenes) associated with the substituents is noted. The possibility of combining colors between the two classes is a technological advantage because it increases the range of possible colors for constructing EDs.

Morphological characterization

Morphological analyses of the thin films/ITO were performed using SEM, as shown in Fig. 5. A lower roughness was observed in the PMOT and P3HT films than in the other films [29]. The films of the PMOT and PEDOT polymers (Fig. 5a, b) have a

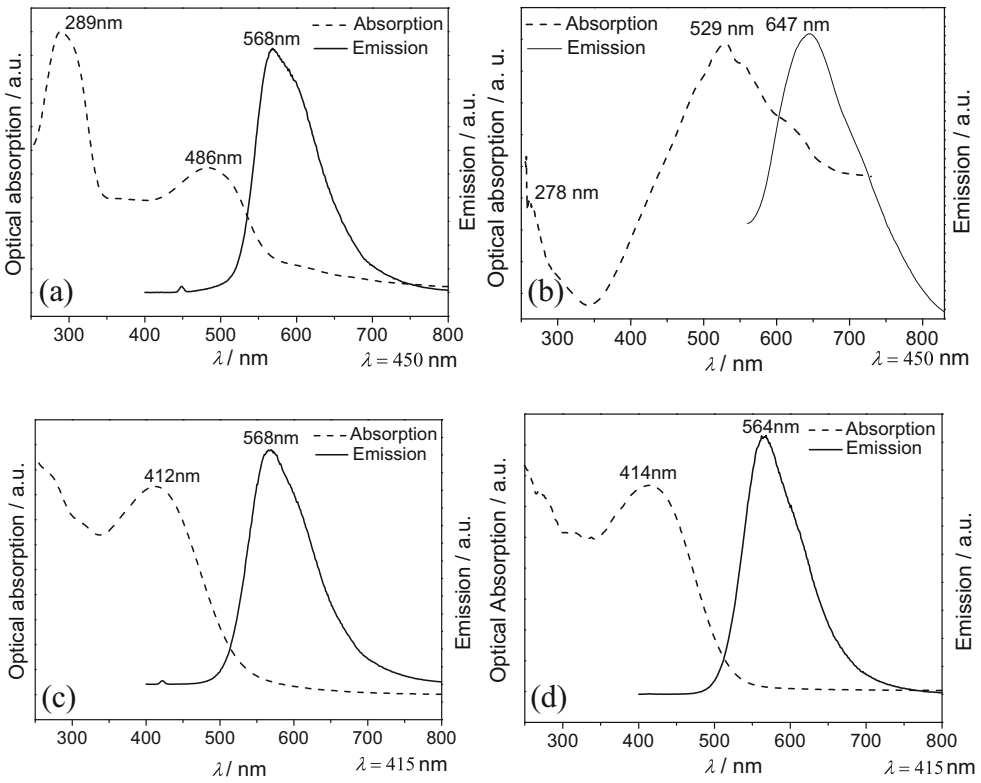

Fig. 4 Absorption and emission spectra obtained by fluorescence spectroscopy for **a** PMOT, **b** PEDOT, **c** P3HT, and **d** PDDT

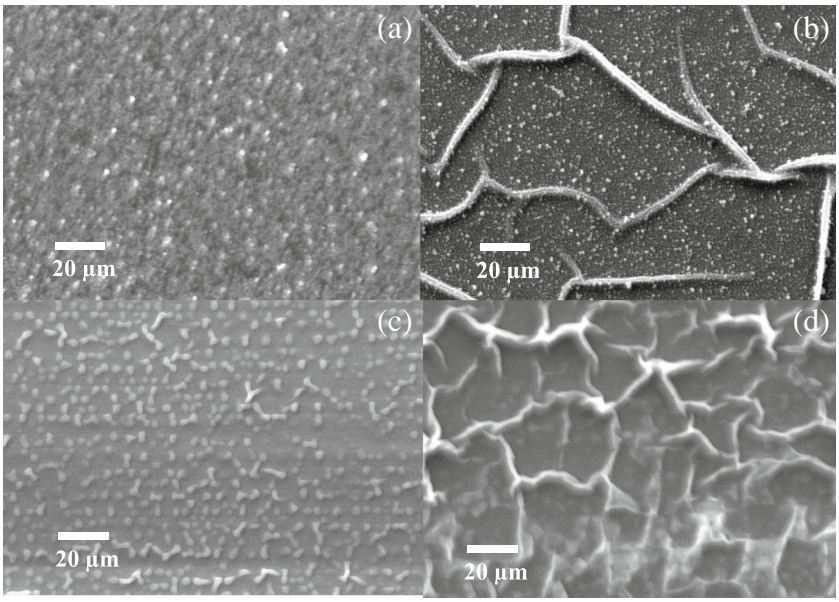

Fig. 5 SEM images from of **a** PMOT, **b** PEDOT, **c** P3HT, and **d** PDDT obtained on a glass/ITO substrate

smooth surface with the presence of typical granules, which can be attributed to the presence of polymer agglomerates in selected regions of the film [30–32].

The P3HT film showed greater homogeneity in the substrate compared with the PDDT film because P3HT formed a flatter surface on the ITO [33–35].

Spectroelectrochemical characterization

To investigate the effects of the deposition method on the average conjugation length of the POT and PYT films, the spectroelectrochemical properties (chemical and electrochemical) of these polymers in the undoped (reduction) and doped (oxides) states were analyzed. In this study, the electron transfer reaction was considered sufficiently fast so that the kinetic limitation during the redox processes can be attributed to the diffusional transport within the film (the kinetics will be limited by mass transport). Thus, lowering the temperature and using a more viscous solvent (nitrobenzene) during electropolymerization was essential for obtaining homogeneous films.

The spectroelectrochemical profile obtained for the polymers is shown in Fig. 6, and the inset in the figure shows the

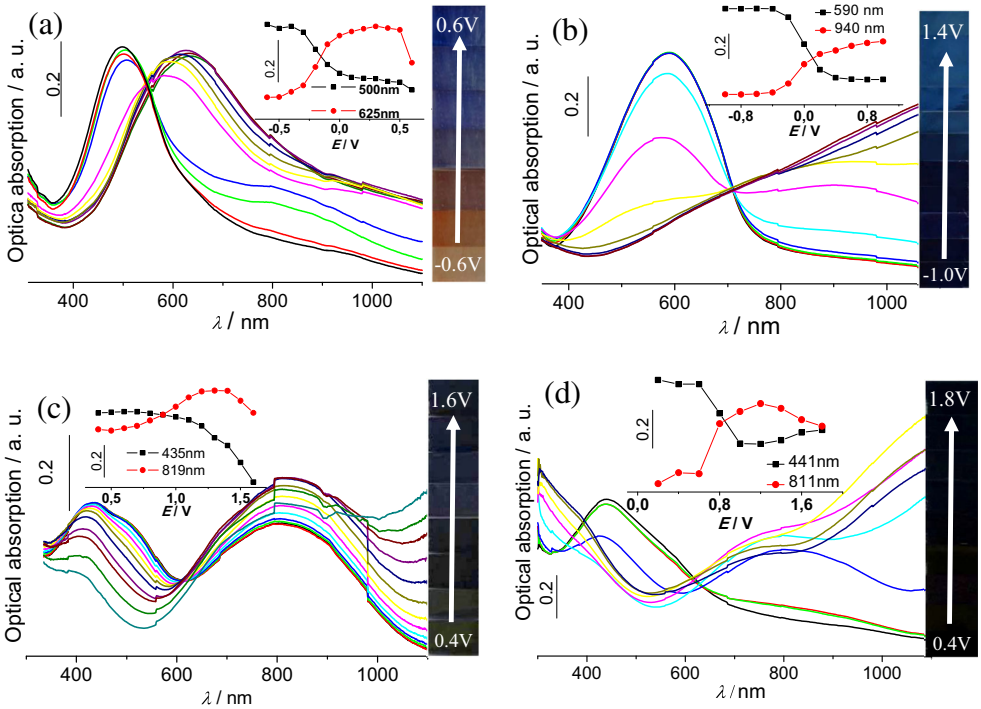

Fig. 6 Spectroelectrochemical analysis of the polymers. Optical absorption curves (OA) at each potential jump for polymers **a** PMOT, **b** PEDOT, **c** P3HT, and **d** PDDT. The details in the graphs show the evolution curves of the optical absorption with the potential applied in the two absorption maxima of the redox states of the polymers. The right-hand side of the figures shows the evolution of the colors of the polymers with the applied potential

Table 2 Summary of spectroelectrochemical data for the polymers

Polymer	Maximum absorption			"Onset"		Inversion point	
	E_{cond}/ V	λ_{max}/ nm	E_{max}/ eV	λ_{tg}/ nm	$E_{\pi\text{-}\pi^*}$/ eV	λ_{in}/ nm	E_{max}/ eV
PMOT	− 0.6	497	2.49	709	1.74	551	2.25
PEDOT	− 0.1	589	2.10	787	1.57	710	1.74
P3HT	0.4	435	2.85	729	1.70	605	2.05
PDDT	0.2	441	2.81	774	1.60	617	2.00

$E_{cond.}$ = conditioning potential; λ_{tg} = wavelength associated with the onset of the BV- > BC as determined by the tangent line to the low-energy region

absorbance curve for two wavelengths (λ), with the first one attributed to the reduced state (λ ~ 480 nm for PYT and λ ~ 550 nm for POT), and the second attributed to the oxidized state (λ ~ 600 nm for PMOT, λ ~ 900 nm for PEDOT, and λ ~ 800 nm for PYT) as a function of the potential. A greater bathochromic shift of λ_{max} occurs for PEDOT than for PMOT, which arises from the increase in the number of oxygen groups in its structure. This phenomenon powerfully demonstrates the contribution of these substituents to increasing the electronic conduction in the polymer chain and favors the bathochromic shift (towards red). The PYTs are influenced by the size of the alkyl substituent chain at the β-position of the thiophene ring, and the increase in the substituent chain contributes to a decrease in energy and the consequent red shift.

The right-hand side of the figures shows the color spectrum of each sample during the potential variation. A gradual decrease of the absorption band at the higher energy and an increase of the absorption band at the lower energy were noted with increasing applied voltage, which was associated with the new intra-gap energy levels of the polaronic state and bipolaronic state formation [35–37]. As expected, all of the films showed a color change from the oxidized state to the reduced state, and this change was reversible in all samples [38]. From the oxidized to the reduced state, the PMOT film changed from blue to orange, PEDOT changed from light blue to dark blue, and P3HT and PDDT changed from dark blue to black.

The values of the energies listed in Table 2 were determined relative to the absorption maximum in the oxidized state, the onset value, and the inversion point. The *onset* of the polaron–bipolaron transitions in the polymers, as determined by tracing a tangent on the low-energy side of the absorption curve, occurs at 1.74, 1.57, 1.70, and 1.60 eV for PMOT, PEDOT, P3HT, and PDDT, respectively.

In the sequence, measurement of the switching time (τ) for the polymers (shown in Fig. 7) was performed using chronoabsorptometry (simultaneous measures of the double step of potential and transmittance as a function of time (s)) [37]. This approach is a relevant method used to evaluate important parameters that supply information for application in EDs, such as coloration efficiency (η):

$$\eta = \frac{\log \frac{\%\mathrm{Tre}}{\%\mathrm{Tox}}}{\mathrm{Q}}$$

where $\%T_{re}$ is the transmittance in the reduced state, $\%T_{ox}$ is the transmittance in the oxidized state, and Q is the total charge. Other parameters are the optical contrast ($\Delta\%T$), for which $\Delta\%T$ is the variation of percentage transmittance ($\%T$)

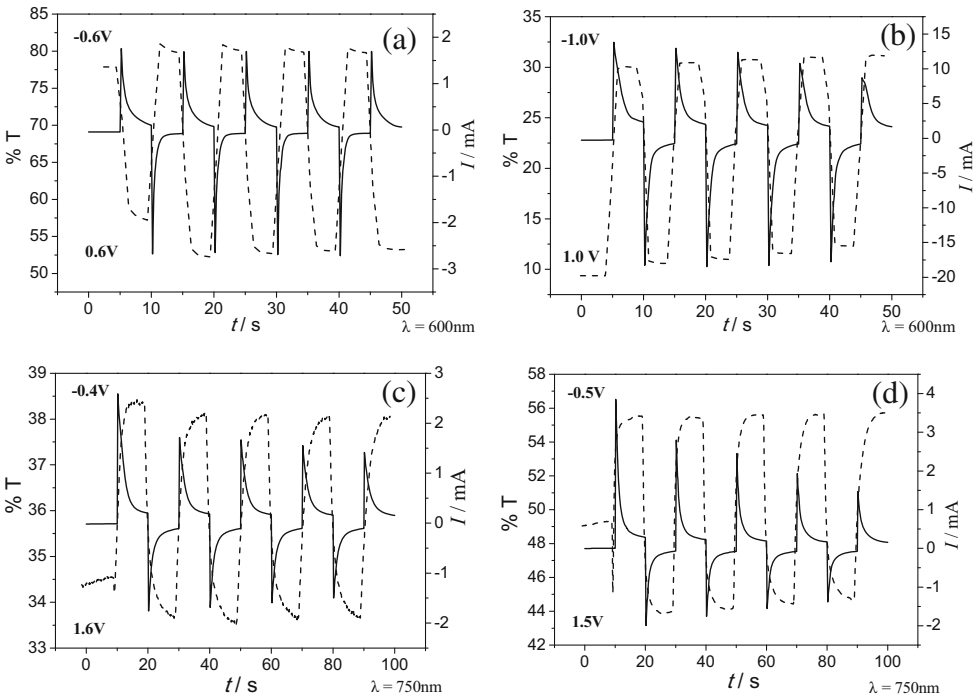

Fig. 7 Optical switching studies for polymers monitored at λ = 600 or 750 nm (solid line, chronoamperogram; dotted line, optical studies): **a** PMOT, **b** PEDOT, **c** P3HT, and **d** PDDT

Table 3 Electrochromic properties of the polymers

Polymer	τ/s		$\Delta\%T$/%	η/cm^2 C^{-1}
	τ_{oxi}	τ_{red}		
PMOT	4.9	2.2	28.5	86.3
PEDOT	3.1	1.8	19.6	12.8
P3HT	9.0	9.3	9.3	4.4
PDDT	6.9	6.5	12.0	3.8

τ: switching time; $\Delta\%T$: optical contrast; η: coloration efficiency

between the reduced and oxidized state [39], and the electrochromic switching time (τ), which is the time required for the material to change color between the redox states. Table 3 shows the electrochromic parameters obtained for the polymers. POT presented better results for the electrochromic properties than PYT. Measurements for the transitions between the reduced and oxidized states showed switching times of 4.9 s (PMOT) and 3.1 s (PEDOT). When the process is reversed between the oxidized and reduced states, the response time increases to 2.2 s for PMOT and 1.8 s for PEDOT. PYT presented a similar switching time for the reduced and oxidized states, namely, ~ 9.0 s (P3HT) and ~ 6.5 s (PDDT).

Interestingly, the polymer with the highest optical contrast ($\Delta\%T$) was PMOT at 28.5%, which is in agreement with the optical and spectroelectrochemical study presented in this work. PMOT also presented variation from red to blue for the change from the oxidized to reduced state. The other polymers presented $\Delta\%T$ values of 10–20%, which indicates a useful system for application in energy-saving windows. The coloration efficiency measurement values for POT are 86.3 cm^2 C^{-1} (PMOT) and 13.0 cm^2 C^{-1} (PEDOT). The coloration efficiency results are influenced by the homogeneity of the deposited films (morphological study, SEM). Compared with the other films, PMOT presented greater homogeneity of the deposited film on the ITO substrate, revealing its effective potential for coloration efficiency. The PEDOT film and the P3HT and PDDT films presented roughness due to the kinetic difficulties of CV deposition, thus influencing the process of load reinjection in the electrochemical reduction process. The electrochromic properties analyzed in this study are promising, and all electrosynthesized polymers are potential candidates for energy-saving window applications [39].

The Coulomb efficiency is defined as $Q_a/Q_c \times 100\%$, where Q_a and Q_c are the anodic and cathodic charges, respectively, determined by the mathematical integration of the anodic and cathodic regions of the chronoamperometry curves (Fig. 7). The values found for the polymers were near 100% for several cycles, indicating that the load consumed in the oxidation process is nearly identical to the load consumption of the reduction process. These data indicate that the redox process occurs virtually completely, and consequently, the color variation occurs reversibly.

Conclusions

In conclusion, we showed that four β-substituted thiophenes (POT and PYT) with electron-withdrawing groups could be easily electrochemically polymerized by CV in a single step from commercially available starting monomers, resulting in the formation of an electroactive conjugated film on the WE. The infrared spectra of the polymers and the electrochemical profiles corroborate these claims.

All of the monomers formed an electroactive polymer film on the ITO-coated glass electrode. These films showed reversible color variation from the reduced state to the oxidized state, namely, from red to blue for the PMOT film, from dark blue to light blue for the PEDOT film, and from dark blue to black for poly(3-alkylthiophenes) films. The polymers exhibit high contrast in the visible region and the formation of new polaronic and bipolaronic energy states. The results show interesting perspectives regarding the use of POT and PYT deposited on ITO/glass electrodes in technological applications.

Acknowledgments This work was supported by CNPq (457586/2014-1), CAPES, FAPEMIG (TEC-APQ-02715-14), and CTNano. We also would like to thank professors Tulio Matencio - UFMG and Marcos Roberto de Abreu Alves - UNIFEI for the important discussions.

References

1. Subramani T, Chen J, Sun Y, Jevasuwan W, Fukata N (2017) Nano energy high-efficiency silicon hybrid solar cells employing nanocrystalline Si quantum dots and Si nanotips for energy management. Nano Energy 35:154–160. https://doi.org/10.1016/j.nanoen.2017.03.037
2. Angaridis PA, Lazarides T, Coutsolelos AC (2014) Functionalized porphyrin derivatives for solar energy conversion. Polyhedron 82:19–32. https://doi.org/10.1016/j.poly.2014.04.039
3. Mortimer RJ (2011) MR41CH10-Mortimer Electrochromic materials. Annu Rev Mater Res 41(1):241–268. https://doi.org/10.1146/annurev-matsci-062910-100344
4. Granqvist CG (2014) Electrochromics for smart windows: oxide-based thin films and devices. Thin Solid Films 564:1–38. https://doi.org/10.1016/j.tsf.2014.02.002
5. Fan M-S, Lee C-P, Vittal R, Ho K-C (2017) A novel ionic liquid with stable radical as the electrolyte for hybrid type electrochromic devices. Sol Energy Mater Sol Cells 166:61–68. https://doi.org/10.1016/j.solmat.2017.03.009
6. Bin GC, He LH, Long JF, Liu LT, Liu S, Tang Q et al (2016) Synthesis and characterisation of azobenzene-bridged cationic-cationic and neutral-cationic electrochromic materials. Synth Met 220:147–154
7. Zhang J, Chen Z, Wang X-Y, Guo S-Z, Dong Y-B, G-A Y et al (2017) Redox-modulated near-infrared electrochromism, electroluminochromism, and aggregation-induced fluorescence change in an indolo[3,2-b]carbazole-bridged diamine system.

Sensors Actuators B Chem 246:570–577. https://doi.org/10.1016/j.snb.2017.02.114
8. Liu H-M, Saikia D, C-G W, Fang J, Kao H-M (2017) Solid polymer electrolytes based on coupling of polyetheramine and organosilane for applications in electrochromic devices. Solid State Ionics 303:144–153. https://doi.org/10.1016/j.ssi.2017.03.005
9. Kiruthika S, Kulkarni GU (2017) Energy efficient hydrogel based smart windows with low cost transparent conducting electrodes. Sol Energy Mater Sol Cells 163:231–236. https://doi.org/10.1016/j.solmat.2017.01.039
10. Kelly FM, Meunier L, Cochrane C, Koncar V (2013) Polyaniline: application as solid state electrochromic in a flexible textile display. Displays 34(1):1–7. https://doi.org/10.1016/j.displa.2012.10.001
11. Chotsuwan C, Asawapirom U, Shimoi Y, Akiyama H, Ngamaroonchote A, Jiemsakul T, Jiramitmongkon K (2017) Investigation of the electrochromic properties of tri-block polyaniline-polythiophene-polyaniline under visible light. Synth Met 226:80–88. https://doi.org/10.1016/j.synthmet.2017.02.001
12. Jensen J, Hösel M, Kim I, JS Y, Jo J, Krebs FC (2014) Fast switching ITO free Electrochromic devices. Adv Funct Mater 24(9):1228–1233. https://doi.org/10.1002/adfm.201302320
13. Groenendaal L, Zotti G, Aubert PH, Waybright SM, Reynolds JR (2003) Electrochemistry of poly(3,4-alkylenedioxythiophene) derivatives. Adv Mater 15(11):855–879. https://doi.org/10.1002/adma.200300376
14. Calado HDR, Matencio T, Donnici CL, Cury LA, Rieumont J, Pernaut JM (2008) Synthesis and electrochemical and optical characterization of poly(3-octadecylthiophene). Synth Met 158(21–24):1037–1042. https://doi.org/10.1016/j.synthmet.2008.07.003
15. Lai JC, Lu XR, Qu BT, Liu F, Li CH, You XZ (2014) A new multicolored and near-infrared electrochromic material based on triphenylamine-containing poly(3,4-dithienylpyrrole). Org Electron Physics, Mater Appl 15(12):3735–3745
16. Kerszulis JA, Amb CM, Dyer AL, Reynolds JR (2014) Follow the yellow brick road: structural optimization of vibrant yellow-to-transmissive electrochromic conjugated polymers. Macromolecules 47(16):5462–5469. https://doi.org/10.1021/ma501080u
17. Zhong YW, Yao CJ, Nie HJ (2013) Electropolymerized films of vinyl-substituted polypyridine complexes: synthesis, characterization, and applications. Coord Chem Rev 257(7–8):1357–1372. https://doi.org/10.1016/j.ccr.2013.01.001
18. Beverina L, Pagani GA, Sassi M (2014) Multichromophoric electrochromic polymers: colour tuning of conjugated polymers through the side chain functionalization approach. Chem Commun (Camb) 50(41):5413–5430. https://doi.org/10.1039/C4CC00163J
19. Liu W, Gu C, Wang J, Sun M, Yang R (2014) Electrochemistry and near-infrared electrochromism of electropolymerized polydithiophenes with β, β'-positions bridged by carbonyl or dicarbonyl substitute. Electrochim Acta 142:108–117. https://doi.org/10.1016/j.electacta.2014.07.111
20. Dietrich M, Heinze J, Heywang G, Jonas F (1994) Electrochemical and spectroscopic characterization of polyalkylenedioxythiophenes. J Electroanal Chem 369(1–2):87–92. https://doi.org/10.1016/0022-0728(94)87085-3
21. Williams DBG, Lawton M (2010) Drying of organic solvents: quantitative evaluation of the efficiency of several desiccants. J Org Chem 75(24):8351–8354. https://doi.org/10.1021/jo101589h
22. Colthup NB, Daly LH, Wiberley SE (1990) Introduction to infrared and Raman spectroscopy. Academic Press, London
23. Szkurlat A, Palys B, Mieczkowski J, Skompska M (2003) Electrosynthesis and spectroelectrochemical characterization of poly(3,4-dimethoxy-thiophene), poly(3,4-dipropyloxythiophene) and poly(3,4-dioctyloxythiophene) films. Electrochim Acta 48(24):3665–3676. https://doi.org/10.1016/S0013-4686(03)00504-8
24. Domagala W, Palutkiewicz D, Cortizo-Lacalle D, Kanibolotsky AL, Skabara PJ (2011) Redox doping behaviour of poly(3,4-ethylenedithiothiophene) - the counterion effect. Opt Mater (Amst) 33(9):1405–1409. https://doi.org/10.1016/j.optmat.2011.02.030
25. Fall M, Assogba L, Aaron JJ, Dieng MM (2001) Revisiting the electropolymerization of 3,4-dimethoxythiophene in organic and micellar media. Synth Met 123(3):365–372. https://doi.org/10.1016/S0379-6779(01)00344-7
26. De Abreu Alves MR, Reis RNC, De Oliveira JG, Calado HDR, Donnici CL, Matencio T (2013) Simultaneous quartz microbalance and mirage effect studies of poly(3-methoxythiophene) electrosynthesis and electrochemical characterisations. Electrochim Acta 105:347–352. https://doi.org/10.1016/j.electacta.2013.04.173
27. Alves MRA, Calado HDR, Donnici CL, Matencio T (2010) Electrochemical polymerization and characterization of new copolymers of 3-substituted thiophenes. Synth Met 160(1–2):22–27. https://doi.org/10.1016/j.synthmet.2009.09.024
28. Rodrigues ADG, Galzerani JC (2012) Espectroscopias de infravermelho, Raman e de fotoluminescência : potencialidades e complementaridades. Rev Bras Ensino Física 34(4):4309–4309
29. Song YJ, Lee JU, Jo WH (2010) Multi-walled carbon nanotubes covalently attached with poly(3-hexylthiophene) for enhancement of field-effect mobility of poly(3-hexylthiophene)/multi-walled carbon nanotube composites. Carbon N Y 48(2):389–395. https://doi.org/10.1016/j.carbon.2009.09.041
30. Dong B, Xu J, Zheng L, Hou J (2009) Electrodeposition of conductive poly(3-methoxythiophene) in ionic liquid microemulsions. J Electroanal Chem 628(1–2):60–66. https://doi.org/10.1016/j.jelechem.2009.01.011
31. Armstrong NR, Carter C, Donley C, Simmonds A, Lee P, Brumbach M, Kippelen B, Domercq B, Yoo S (2003) Interface modification of ITO thin films: organic photovoltaic cells. Thin Solid Films 445(2):342–352. https://doi.org/10.1016/j.tsf.2003.08.067
32. Lee H, Lee J, Park S-M (2010) Electrochemistry of conductive polymers 45. Nanoscale conductivity changes of PEDOT : PSS films studied by current-sensing atomic force microscope (CS-AFM). J Phys Chem B 114(8):2660–2666. https://doi.org/10.1021/jp9113859
33. Han Z, Zhang J, Yang X, Cao W (2011) Synthesis and application in solar cell of poly(3-octylthiophene)/cadmium sulfide nanocomposite. Sol Energy Mater Sol Cells 95(2):483–490. https://doi.org/10.1016/j.solmat.2010.09.006
34. Singh RK, Kumar J, Kumar A, Kumar V, Kant R, Singh R (2010) Poly(3-hexylthiophene): functionalized single-walled carbon nanotubes: (6,6)-phenyl-C61-butyric acid methyl ester composites for photovoltaic cell at ambient condition. Sol Energy Mater Sol Cells 94(12):2386–2394. https://doi.org/10.1016/j.solmat.2010.08.023
35. Chen X, Inganäs O (1996) Three-step redox in Polythiophenes: evidence from electrochemistry at an Ultramicroelectrode. J Phys Chem 100(37):15202–15206. https://doi.org/10.1021/jp9601779
36. Brédas JL, Scott, Yakushi K, Street GB (1984) Polarons and bipolarons in polypyrrole: evolution of the band structure and optical spectrum upon doping 30(2):1023–5
37. Sacan L, Cirpan A, Camurlu P, Toppare L (2006) Conducting polymers of succinic acid bis-(2-thiophen-3-yl-ethyl)ester and their electrochromic properties. Synth Met 156(2–4):190–195. https://doi.org/10.1016/j.synthmet.2005.11.010
38. Damlin P, Kvarnström C, Ivaska A (2004) Electrochemical synthesis and in situ spectroelectrochemical characterization of poly(3,4-ethylenedioxythiophene) (PEDOT) in room temperature ionic liquids. J Electroanal Chem 570(1):113–122. https://doi.org/10.1016/j.jelechem.2004.03.023
39. Krishnamoorthy K, Kanungo M, Contractor AQ, Kumar A (2001) Electrochromic polymer based on a rigid cyanobiphenyl substituted 3,4-ethylenedioxythiophene. Synth Met 124(2–3):471–475. https://doi.org/10.1016/S0379-6779(01)00396-4